

The nature of the faint galaxies in the Hubble Deep Field

B. Mobasher, M. Rowan-Robinson, A. Georgakakis, N. Eaton

Astrophysics Group, Blackett Laboratory, Imperial College, Prince Consort Rd, London SW7 2BZ

9 September 2021

ABSTRACT

We present a study of the galaxies found in the Hubble Deep Field. A high proportion of HDF galaxies are undergoing a strong episode of star formation, as evidenced by their very blue colours. A wide range of morphological types is found, with a high proportion of peculiar and merger morphologies.

Fitting the multiband spectra with redshifted SEDs of galaxy types E to III, we predict the spectral types and redshifts of galaxies detected in the HDF. We find a median redshift of 1.6, with 68% having $z > 1$ and 31% with $z > 2$. The I-band absolute magnitude distributions as a function of galaxy types show a plausible trend of decreasing luminosity towards later types. The derived I-band luminosity function agrees well with that from the Canada-France survey (Lilly et al 1996) for $z < 1$ and shows strong luminosity evolution at $M_I < -21$ for $1 < z < 3$, comparable to the rate seen in quasars and starburst galaxies.

We have predicted infrared and submillimetre fluxes assuming most of the galaxies are undergoing a strong starburst. Several planned space-borne and ground-based deep surveys are capable of detecting interesting numbers of HDF galaxies.

Key words:

1 INTRODUCTION

In December 1995 an area of five square arcminutes at RA 12h 36m 49.4s Dec +62 12 58 (J2000) was surveyed by the Hubble Space Telescope to an unprecedented depth (Williams et al 1996). This survey, referred to as the Hubble Deep Field (HDF), consists of three wide field areas, each of size 75 arcsec square, carried out by the WFPC2, and a smaller area of 35 arcsec square covered by the planetary camera. The HDF is over one magnitude deeper than the deepest surveys previously done by the HST and is carried out in four bands; F300W(300nm), F450W(450nm), F606W(600nm) and F814W(800nm), roughly corresponding to the UBVI system. The field is chosen to have a representative number density for galaxies and be devoid of bright stars.

One of the main applications of the HDF is to study the nature of the faint population of galaxies found in ground based optical surveys. Recent models, interpreting deep counts of galaxies, have invoked bursts of star formation, merging of galaxies (Broadhurst et al 1988), dust obscuration (Franceschini et al 1994), the presence of a new population of dwarf galaxies (Cowie et al 1990) and a steep faint-end slope for the local luminosity function (Koo et al 1993). The degree to which we can discriminate between these competing scenarios is limited by the size and depth of the available surveys, the morphological type information obtained from them at deep levels and the wavelength in

which they have been carried out. The HDF and its follow up spectroscopic observations are expected to disentangle some of these scenarios and provide a natural extension to ground-based optical surveys (Smail et al 1995, Lilly et al 1996). Recently, Abraham et al (1996) performed morphological type classification of the HDF galaxies with $I < 25$ mag and conclude that at this depth, the classical Hubble system fails to explain the large fraction of peculiar/Irregular/merger galaxies observed in the HDF.

In this study, we explore the nature of the faint galaxy population observed in the HDF. Using the available multi-wavelength information, we predict photometric redshifts and spectral types of the galaxies detected in the HDF. These are used to make a preliminary study of the distribution of the faint blue population in redshift and luminosity space. A promising aspect of future studies of the HDF is follow-up at longer infrared and sub-millimetre wavelengths. We make predictions of the fluxes expected at these wavelengths, assuming most of the galaxies are undergoing a major episode of star formation. We assume $H_0 = 50$ km/sec/Mpc and $q_0 = 0.5$ throughout this paper.

The catalogue generation is discussed in the next section. Section 3 presents a study of the faint blue galaxy population in the HDF, followed by estimates of photometric redshifts and spectral types of the galaxies in section 4. The Hubble diagram and luminosity function of the HDF galaxies are presented in section 5, and prediction of their

arXiv:astro-ph/9604118v2 30 Apr 1996

infrared and submillimetre fluxes in section 6. Conclusions are summarised in section 7.

2 CREATION OF A GALAXY CATALOGUE

Independent galaxy catalogues were first generated in all the four bands. Object identifications and star/galaxy separations were performed, using the PISA software in the STARLINK environment. This was further confirmed using the FOCAS/IRAF source identification package. Aperture photometry was then carried out with PHOTOM on all the identified galaxies, using an aperture size of $0.5''$ diameter. For $0.5 < z < 3$, this corresponds to a linear diameter of $4.0 \pm 0.2 (h/50)^{-1}$ kpc. The photometry zero points provided by the STScI were used. The catalogues for different bands were cross correlated and objects with detections in more than one band were identified. A total of 1761 galaxies were identified in the 3 WFPC2 fields, of which 1536 were detected in the I-band. 327 galaxies have been detected in all four bands, 577 in the 3 bands (IVB), 397 in the 2 bands (IV), while 230 were detected in one band only (the I band in the case of 229 galaxies). A total of 1307 galaxies were detected in both I and V bands (and in other bands for 910 objects). This sample forms the basis of the present study, ie. we ignore the 230 single band detections. The magnitudes at which serious incompleteness sets in are $I \sim 28$, $V \sim 28.5$, $B \sim 28.5$, $U \sim 26$, with the completeness limit for statistical purposes being about 0.5 magnitudes brighter than these values.

Morphological type classification of galaxies detected in four bands was carried out by two of us (AG and BM). Galaxies were divided into four categories; ellipticals, spirals, irregular/peculiar and mergers, the latter being defined as objects with multiple nuclei.

3 THE FAINT BLUE GALAXY POPULATION IN THE HDF

The (B-V)-(U-B) colour-colour diagram for different morphological types of galaxies, detected in all 4 bands, are compared with model predictions in Fig. 1. The synthetic colours are predicted at different redshifts using the observed SEDs of elliptical, spiral (Sbc) and HII galaxies. The SEDs of elliptical and spiral galaxies are taken from Yoshii and Takahara (1986) and that for the HII galaxies is from the observed continuum of Tol 1924-416 (Calzetti and Kinney (1992)). The study of the UV continua of HII galaxies by Kinney (1993) indicates that the UV spectrum of this galaxy is typical of HII galaxies. The predicted colours for $z > 1.5$ are based on extrapolation of the observed/model continua to the Lyman limit, beyond which we assume the continua to drop steeply. The predicted colours are calculated in the HST filters.

The striking feature in Fig. 1 is the presence of two different branches with similar U-B but different B-V colours. The irregular/peculiar galaxies lie at the blue end of the colour-colour diagram with the merging galaxies extending to the blue branch, presumably due to star formation induced by galaxy mergers.

The range of predicted colours agree with the observed

data. The blue branch is reasonably well fitted by the elliptical and HII galaxy models, shifted to high redshifts ($z \sim 1.5 - 2$) for the very blue galaxies. At these redshifts, the $U - B$ colours rapidly increase as the Lyman limit comes into the U-band. Also, the spiral galaxy locus and the red part of the HII galaxy model are in fairly good agreement with the observed data in the range $z = 0 - 0.5$.

4 PHOTOMETRIC REDSHIFT ESTIMATES

Since most of the HDF galaxies are too faint for spectroscopic redshift measurements with even the largest ground-based telescopes, it is useful to estimate their photometric redshifts, using the available multi-wavelength data. The existence of the U-band data, covering the 4000 Å break is crucial for such purpose (Connolly et al 1995; Koo 1986).

The observed, rest frame SEDs for 6 different types of galaxies (E/SO, Sab, Sbc, Scd, Sdm from Yoshii and Takahara 1986 and HII from Calzetti and Kinney 1993, as above) are used to produce a grid of SEDs in the $\log(1+z)$ range 0.01 to 0.6 in 0.01 intervals. These are then compared with the observed SEDs for the HDF galaxies and the best fit was selected by least squares. The corresponding redshift and spectral type was then associated with that galaxy. The agreement between the spectral and morphological type classification was found to be better than 75 percent. We find that the number of galaxies of SED-type E/SO, Sab, Sbc, Scd, Sdm and HII are 219, 193, 81, 169, 285, 366 respectively.

The uncertainty in the redshift can be estimated by calculating the value of χ^2 as a function of z for each galaxy type. For an assumed magnitude error of 0.06 mag. in each band, the typical uncertainty in $(1+z)$ ranges from 3 - 10% for a galaxy detected in all 4 bands, with only a minority giving acceptable solutions for more than one galaxy type. However, for objects detected in only 3 or 2 bands, the uncertainty in redshift increases and there is often more than one acceptable redshift/galaxy type solution. The redshift distribution for the whole sample is shown (as a function of galaxy type) in Fig 2. No obvious bias is present and on the whole, there is smooth distribution of redshifts for each galaxy type. The strong peaks at $z = 2$ and $z = 3$ are probably artefacts of the photometric redshift method and a result of our ignorance of the far-UV properties of galaxies. To explore the sensitivity of our results to selection effects and redshift errors, we also consider the redshift distributions for galaxies detected in all the 4 bands (Fig.2- dotted line). These galaxies, which have more accurate redshifts, follow the redshift distribution, based on all the objects, producing again a peak at $z \sim 2$.

There are 109 objects which are detected in B, V, I bands but not in the U-band, and for which the U-band limit ($U < 26.5$) implies $f_\lambda(U) < f_\lambda(B)$. For these, we set $U = 26.5$ mag., resulting to a redshift in the range 1.9-2.2 and for many of these cases, to a much higher redshift, up to 3.5. Also, there are 9 galaxies detected only in the I and V bands, with blue (V-I) colours, but for which the non-detection in the U- and B-bands implies a significant drop in the observed blue continuum. These are candidates for the Lyman limit being redshifted into the blue band, so that they would be expected to have $z \geq 3.6$. These are obvious candidates for future spectroscopic observations.

The I-band absolute magnitude distribution M_I for each galaxy type are presented in Fig 3. These show a highly plausible trend of decreasing absolute magnitude towards later type galaxies. The absolute magnitude distribution, based on galaxies with more accurate redshifts (ie. those detected in all the 4-bands), are also presented (Fig. 3-dotted line) and show a similar trend with type. This indicates that the increase in errors in redshifts for some of the objects here does not affect the main results of this study.

5 I-BAND HUBBLE DIAGRAM AND LUMINOSITY FUNCTION

The I-band Hubble diagrams for the whole HDF galaxy sample is shown in Fig 4a, together with the predicted curves for an Sbc galaxy with $M_I = -20$. This diagram is a natural extension to fainter magnitudes of the corresponding distribution found by Crampton et al (1996) for the Canada-France survey to $I = 22.5$ (their Fig 4). The corresponding Hubble diagram for the 327 galaxies detected in all the four bands is shown in Fig 4b, with morphological types indicated by different symbols. There is a clear trend towards fainter magnitudes with increasing redshift, suggesting the photometric redshifts are reasonable. An even clearer trend emerges when only galaxies with elliptical spectral-types are plotted (Fig 4c), as expected from the smaller scatter in their absolute magnitudes (Fig 3).

The I-band completeness limit of the HDF is estimated as $I = 27.5$ mag. For the 1148 galaxies brighter than this limit, we have calculated the luminosity function in three different redshift intervals (Fig 5). The luminosity function for $z < 1$ shows remarkably good consistency with that found by Lilly et al (1996) for the Canada-France survey to $I = 22.5$ mag. They agree both in the normalisation and in the steep faint end slope, which we find to be $\alpha = 1.5$ at $M_I > -22$, caused mainly by Sdm and HII galaxies. At $M_I < -21$, there is clear evidence for strong evolution in the luminosity function, with approximately a similar rate for the luminosity evolution as found for quasars (Boyle et al 1988) and starburst galaxies (Saunders et al 1990, Rowan-Robinson et al 1993, Oliver et al 1995, Rowan-Robinson 1996). Although some optical galaxy redshift surveys have claimed to be inconsistent with luminosity evolution (Broadhurst et al 1988, Colless et al 1990), recent studies have begun to find hints of luminosity evolution in the galaxy luminosity function (Colless 1995, Lilly et al 1996). A study of the type-dependence of the luminosity function here shows that their faint end are mainly dominated by late-type spirals and HII galaxies (ie. galaxies undergoing star formation and luminosity evolution).

6 PREDICTION OF INFRARED AND SUBMILLIMATRE FLUXES

It is a goal for many space projects and ground-based telescopes, existing or planned in the infrared and submillimetre (eg ISO, SCUBA, FIRST, MMA/LSA), to detect starburst galaxies at high redshift. It is therefore of great interest to predict the infrared and submillimetre fluxes for the HDF galaxies.

The very blue colours of most of the HDF galaxies suggest that they are undergoing a strong episode of star formation, and this is supported by the high incidence of peculiar and merging morphologies. We assume that the SEDs of these galaxies at infrared and submillimetre wavelengths can be well represented by the standard starburst model of Rowan-Robinson and Efstathiou (1993). For the relative normalisation between far-infrared and optical, we make an assumption similar to that made by Pearson and Rowan-Robinson (1996), namely that $F = \nu S_\nu(60\mu m)/\nu S_\nu(0.8\mu m) = 10$ in the rest-frame. These authors claim that if the proportion of the total bolometric power in a starburst, emerging in the optical-uv, is greater than about 5 – 10%, then the optical galaxy counts at $B = 21 - 23$ mag. would be violated.

With these assumptions, we predict the flux for HDF galaxies at infrared or submillimetre wavelength, allowing for their redshift and galaxy type. Table 1 gives the number of HDF galaxies expected brighter than a given flux-density at wavelengths of interest to ISO, SCUBA, FIRST and proposed large millimetre arrays (LSA/MMA). It appears that deep integrations by the ISO, SCUBA and FIRST are capable of detecting a number of HDF galaxies.

We have also calculated the total background intensity expected from these galaxies at each wavelength (see Table 1). The resulting spectrum is similar in shape and amplitude to that predicted by Pearson and Rowan-Robinson (1996, see also Oliver et al 1992, Rowan-Robinson and Pearson 1996), consistent with the picture that the majority of these galaxies are strongly evolving starbursts, previously studied in far-infrared and sub-mJy radio surveys.

7 CONCLUSIONS

The conclusions of this study can be summarized as follows:

- (i) A high proportion of HDF galaxies are undergoing a strong episode of star formation, as evidenced by their very blue colours. A wide range of morphological types is found, with a high proportion of peculiar and merger morphologies.
- (ii) Fitting the multiband spectra with redshifted SEDs of galaxy types E to HII, gives a plausible distribution of galaxy types, redshifts and absolute magnitudes. We find a median redshift of 1.6, with 68% having $z > 1$ and 31% $z > 2$. The I-band absolute magnitude distributions as a function of galaxy types show the expected trend of decreasing luminosity towards later type galaxies.
- (iii) The derived I-band luminosity function agrees remarkably well with that from the Canada-France survey (Lilly et al 1996) for $z < 1$ and shows strong luminosity evolution at $M_I < -21$ for $1 < z < 3$, comparable to the rate seen in quasars and starburst galaxies.
- (iv) We have predicted the infrared and submillimetre fluxes assuming most of the galaxies are undergoing a strong starburst. Several planned space-borne and ground-based deep surveys are capable of detecting interesting numbers of HDF galaxies.

Table 1. Predicted cumulative numbers of HDF galaxies as a function of infrared and submillimetre flux-densities

wavelength:	6.7	15	60	90	200	400	800	1200 μm
flux-density:								
10 mJy	0	0	0	0	4	1	0	0
1mJy	0	0	2	14	85	52	4	0
100 Jy	1	7	93	263	403	325	121	37
10 Jy	15	161	522	763	975	698	400	295
1 Jy	737	1218	1307	1307	1307	1296	1155	1054
lg (background intensity) ($Wm^{-2}sr^{-1}$)	-8.91	-8.48	-8.31	-8.04	-7.85	-8.40	-9.39	-10.02

REFERENCES

- Abraham R. G., Tanvir N. R., Santiago B. X., Ellis R. S., Glazebrook K., van den Bergh S., 1996, MNRAS (in press)
- Broadhurst T.J., Ellis R.S., Shanks T., 1988, MNRAS 235, 837
- Calzetti, Kinney, 1992, ApJ 399, L39
- Colless M.M., Ellis R.S., Taylor K., Hook R.N., 1990, MNRAS 244, 408
- Colless M., 1995, in 'Wide Field spectroscopy and the Distant Universe', eds S.J.Maddox and A.Aragon-Salamanca (World Scientific, Singapore), p.263
- Connolly A., Csabai I., Szalay A.S., Koo D.C., Kron R.G., Munn J.A., 1995, AJ 110, 2655
- Cowie L., 1990, Physicsl Cosmology, 79th Nobel Symposium, Physica Scripta
- Crampton D., Le Fevre O., Lilly S.J., Hammer F., 1996, preprint
- Franceschini A., Mazzei P., De Zotti G., Danese, L., 1994, ApJ 427, 140
- Kinney, 1993, ApJ Supp 86, 5
- Koo D.C., Gronwall C., Bruzual A.G., 1993, ApJ 415, L21
- Koo D.C., 1986, AJ 90, 418
- Lilly S.J., Tresse L., Hammer F., Crampton D., Le Fevre O., 1996, preprint
- Oliver S.J., Rowan-Robinson M., Saunders W., 1992, MNRAS 256, 15p
- Pearson C., Rowan-Robinson M., 1996, MNRAS in press
- Rowan-Robinson M., 1996, in 'Cold Gas at High redshift'
- Rowan-Robinson M., Efstathiou A., 1993, MNRAS 263, 675
- Rowan-Robinson M., Benn C.R., Lawrence A., McMahon R.G., Broadhurst T.J., 1993, MNRAS 263, 123
- Rowan-Robinson M., Pearson C., 1996, in 'Unveiling the Cosmic Infrared Background', ed. E.Dwek ((American Institute of Physics: New York), p.192
- Smail I., Hogg D.W., Yan L., Cohen J., 1995, ApJ 449, 105
- Williams, R.E. et al 1996, Science with the Hubble Space Telescope- II, eds, Benvenuti, P., Macchetto, F.D., Schreier, E.J., STScI, In press
- Yoshii Y., Takahara F., 1988, ApJ 326, 1

Figure Captions

Fig 1: (B-V) v. (U-B) for 327 HDF galaxies detected in all 4 bands. Predicted loci as a function of redshift, for $0 < z < 3$, are shown for E (...), Sbc (---) and HII (---) galaxies.

Fig 2: Redshift distribution as a function of galaxy spectral types. The peaks at $z = 2$ and 3 are likely artefacts of the photometric redshift method and our lack of knowledge of the far-UV spectra of galaxies. Distributions for the objects detected in all the 4 bands are plotted in dotted lines.

Fig 3: Absolute magnitude distribution as a function of galaxy spectral type. There is a plausible trend of decreasing peak luminosity towards later types. Distributions for the objects detected in all the 4 bands are plotted in dotted lines.

Fig 4: (a) I-band Hubble diagrams for the whole sample (1307 galaxies). The 9 galaxies with blue $V - I$ colours, detected only in I and V bands, are also plotted at a redshift of 3.57. These are candidates for high redshift objects. (b) I-band Hubble diagram for HDF galaxies detected in all 4 bands; E/SO (\bullet); Sa/Sab (\star); Sb/Sbc (\ast); Sc/Scd (\circ); Sd/Sdm (\times); HII (\square). (c) I-band Hubble diagram for elliptical galaxies. The lines are the predicted relations for $M_I = -20$ mag.

Fig 5: I-band luminosity function for 3 redshift ranges. Note the steep faint end slope ($\alpha = 1.5$) caused mainly by Sdm and HII galaxies and the strong luminosity evolution for $M_I < -21$ mag.

Figure 1.

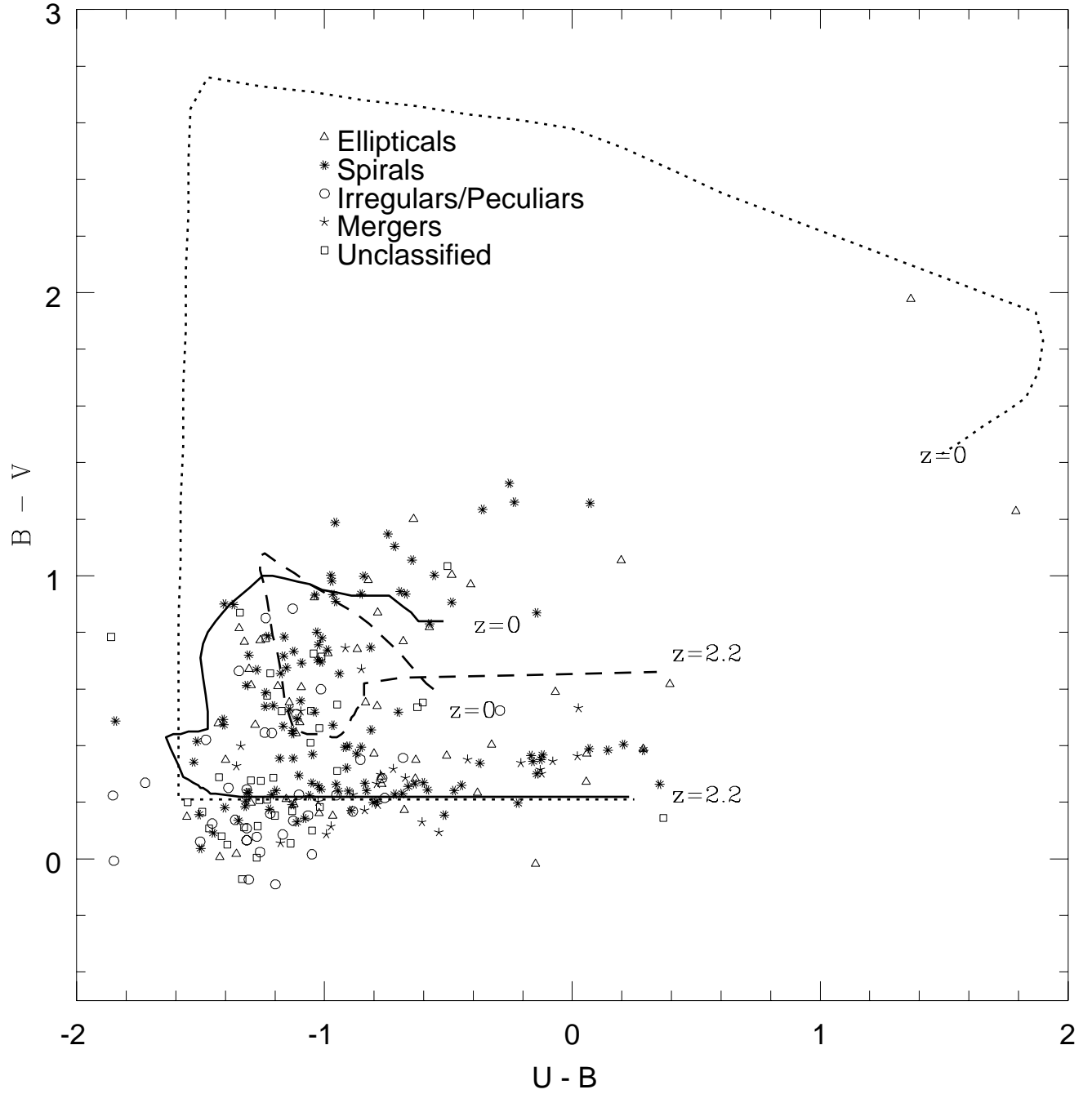


Figure 2.

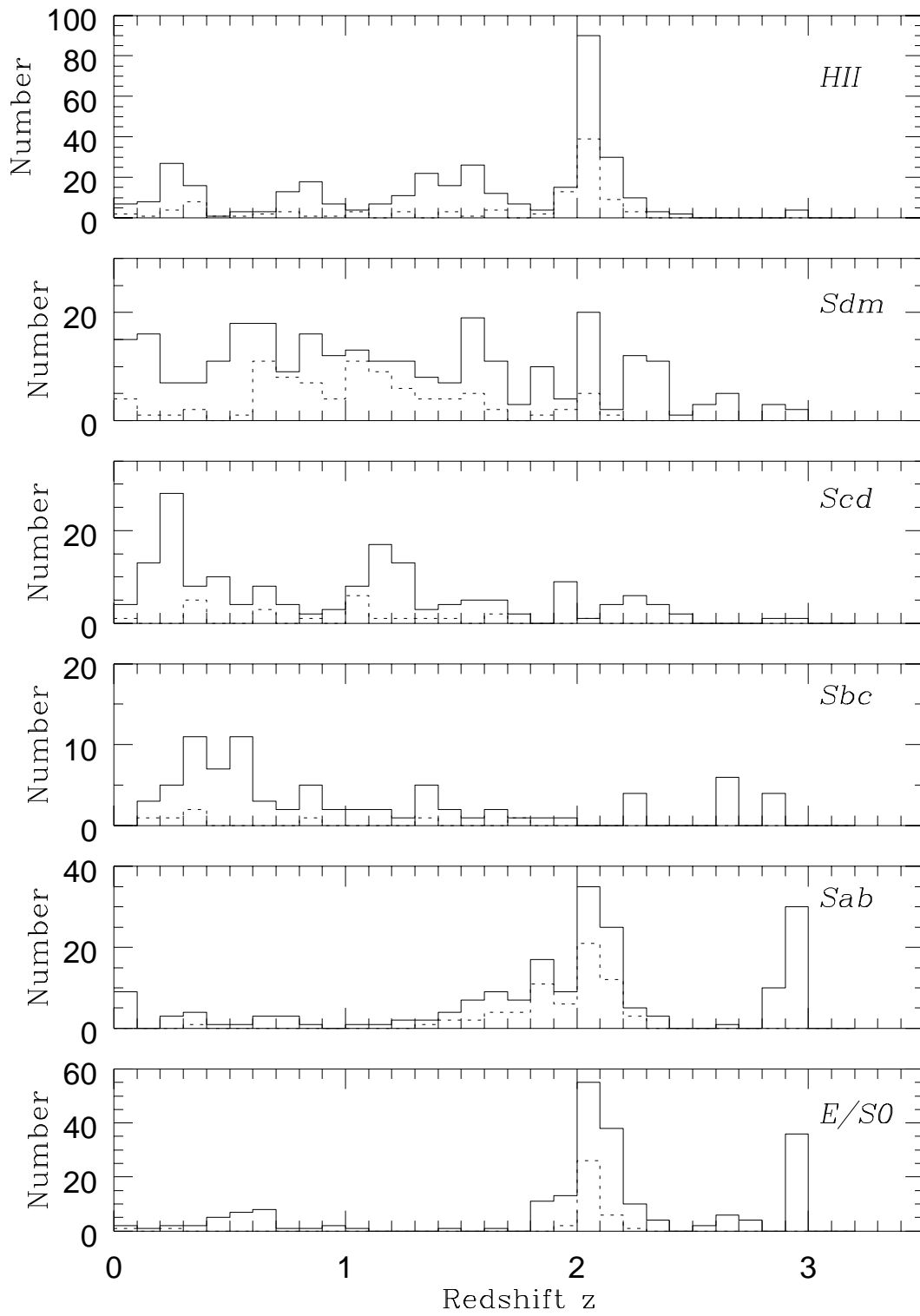


Figure 3.

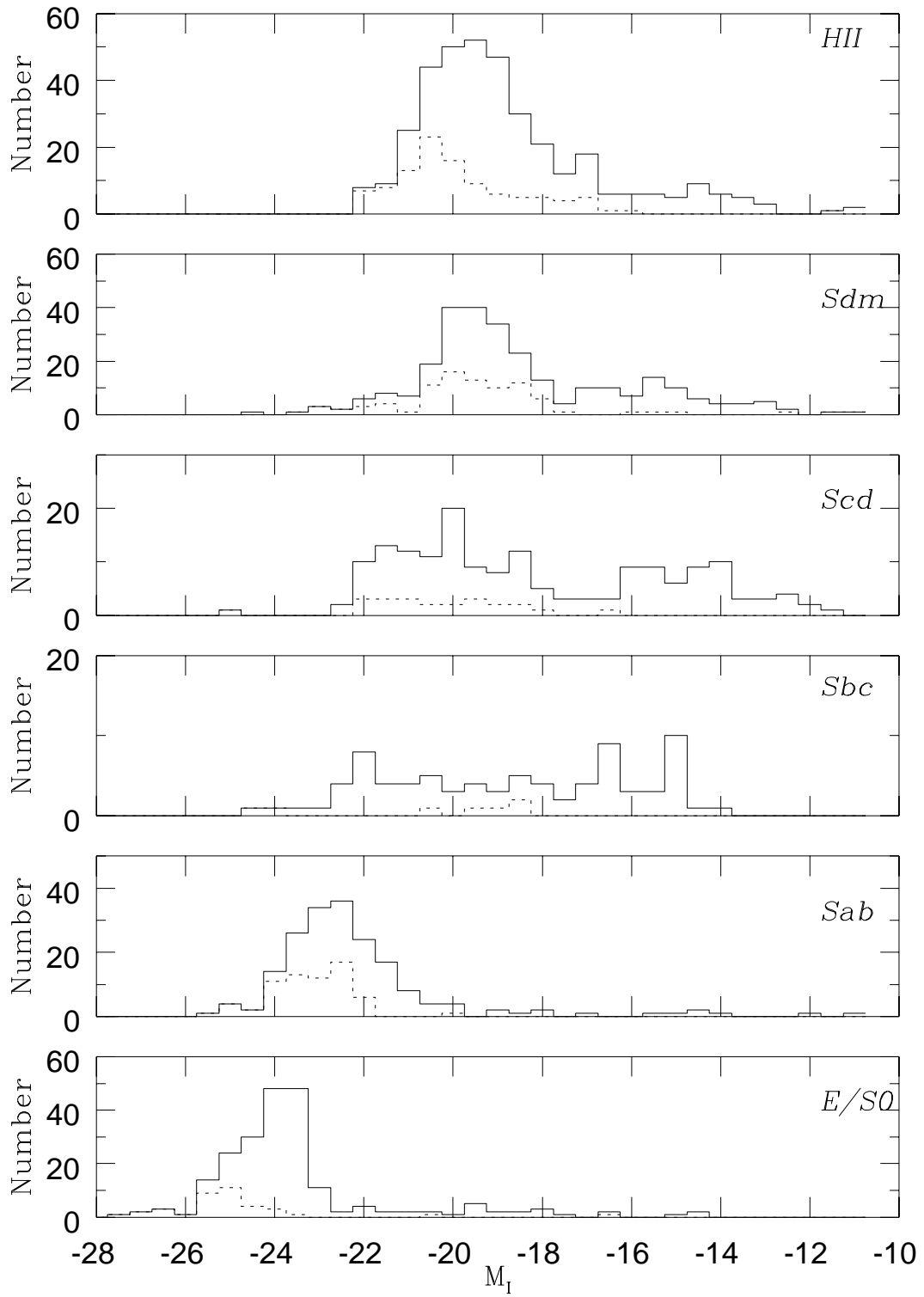


Figure 4.

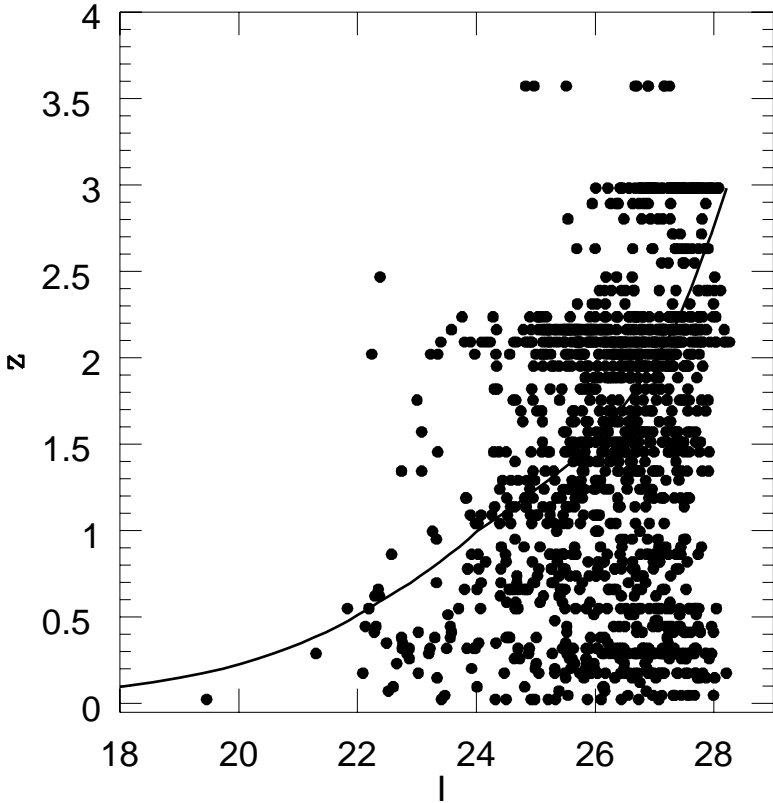


Figure 5.

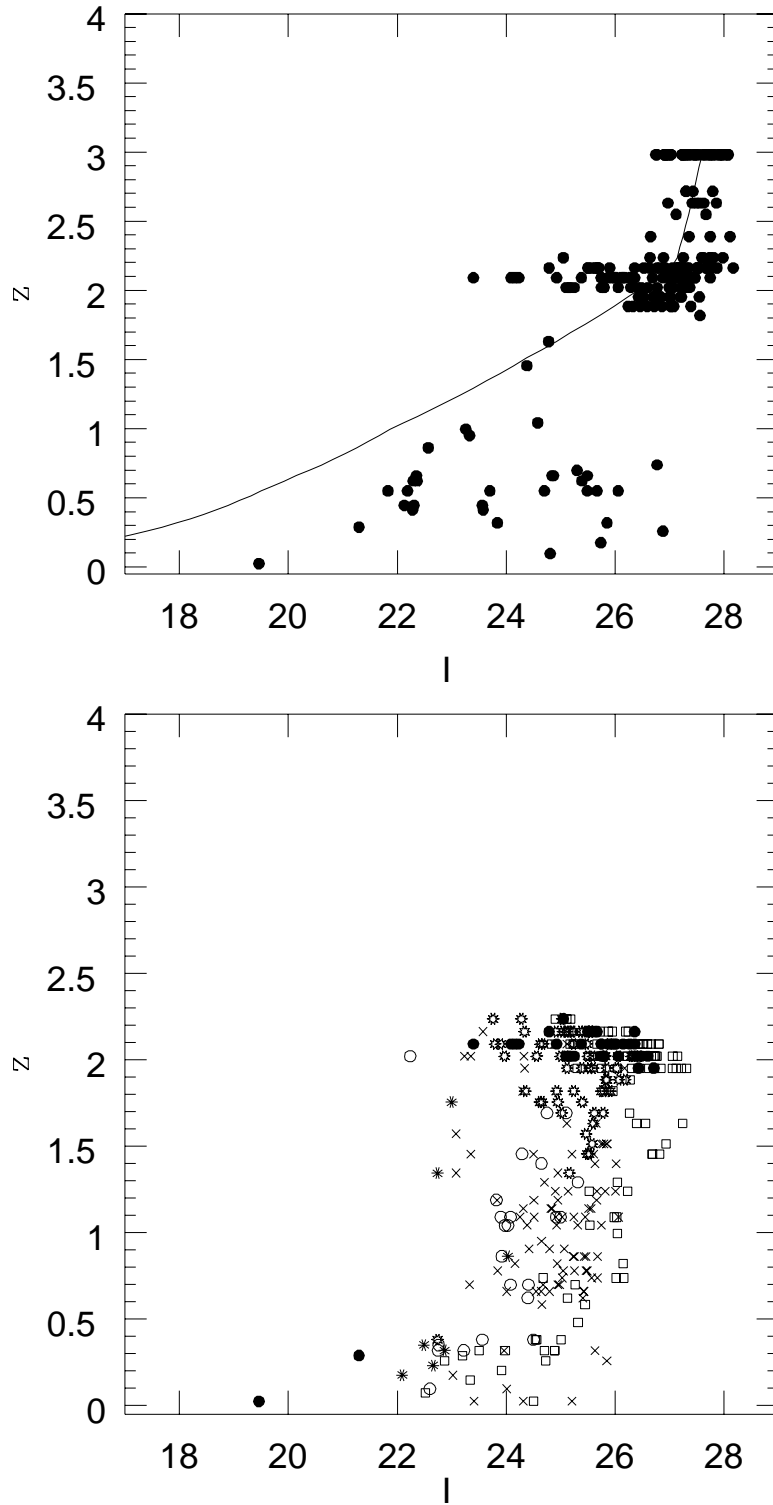


Figure 6.

